RSC Advances

ROYAL SOCIETY OF CHEMISTRY

www.rsc.org/advances
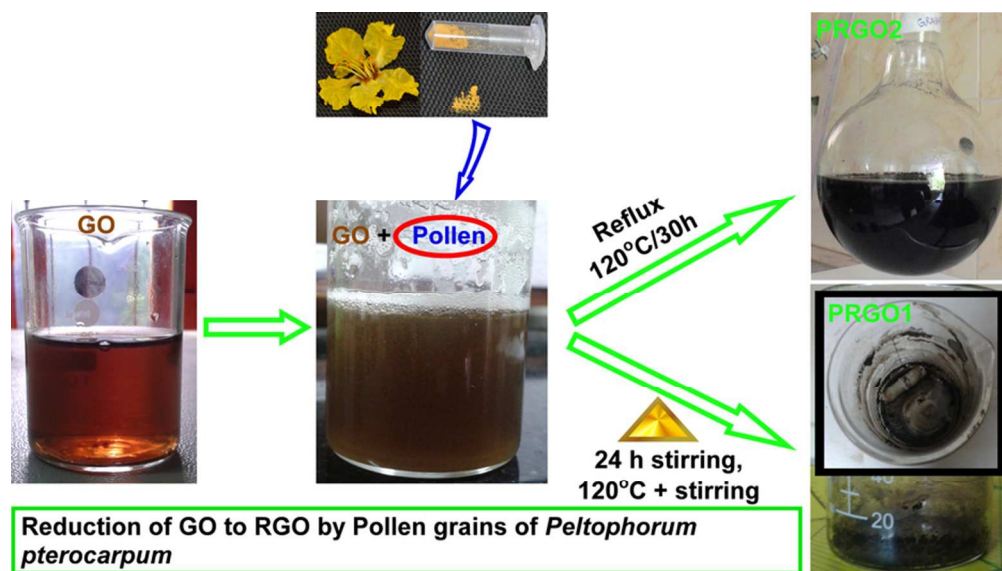
39x22mm (600 x 600 DPI)

A facile green synthesis of reduced graphene oxide by using pollen grains of *Peltophorum pterocarpum* and its electrochemical behavior

O. S. Asiq Rahman[1], V. Chellasamy[1], N. Ponpandian[2], S. Amirthapandian[3], B. K. Panigrahi[3], P. Thangadurai[1,*]

[1]Centre for Nanoscience and Technology, Pondicherry University, Kalapet, Puducherry – 605 014, India

[2]Department of Nanoscience and Technology, Bharathiar University, Coimbatore – 641 046, India

[3]Ion beam and computer simulation section, Materials Science Group, Indira Gandhi Centre for Atomic Research, Kalpakkam – 603 102, India

Corresponding Author: Email: thangaduraip.nst@pondiuni.edu.in
Phone: +91-413-2654974
Fax: +91-413-2656758

Abstract

Reduced graphene oxide (RGO) was prepared from graphite oxide (GO) by using pollen grains (Pgs) of *Peltophorum pterocarpum* as reducing agent and studied their electrochemical behavior. The RGOs were also prepared without and hydrazine hydrate as reducing agent for comparison. All the RGOs were studied by x-ray diffraction, Raman and FTIR spectroscopies. Microstructure was studied by scanning and transmission electron microscopies and the phase formation was further confirmed by electron energy loss spectroscopy. The reduction by the Pgs was comparable to the same as hydrazine hydrate. Cyclic voltammetry studies showed good electrochemical performance of RGO with the maximum specific capacitance of 27.1 Fg^{-1} (for the scan rate of 5 mVs^{-1}). This synthesis method is reported to be *Green* due to a non-hazardous nature of Pgs to the environment and economic.

Keywords: Graphite oxide; Reduced graphene oxide; Peltophorum pterocarpum; Green reduction; pollen grains; Cyclic voltammetry

1

1. Introduction

Graphene is a two dimensional sp^2 hybridized with single atomic thickness of carbon layers [1] and different from fullerenes and carbon nanotubes. A single and a few layers of graphene exhibits excellent properties including high surface area as well as excellent chemical, electrical, thermal and mechanical properties. Mostly, carbon materials such as activated carbon, mesoporous carbon, carbon aerogel, carbon nanotubes are used as electrode material for electrochemical double layer capacitor because of high surface area and low cost. Recently, numerous applications of graphene have been reported and very importantly in the development of electrochemical energy conversion and storage devices including supercapacitors and electrochemical double layer capacitors [2-5]. In the case of supercapacitors, they are low cost, possess longer cycle-life, experience no memory effect, require a very simple charging circuit, and are generally much safer than batteries. Graphene and its nanocomposites have become potential electrode materials because of their high theoretical specific surface area ($2630 \ m^2g^{-1}$) and electrical conductivity.

Large scale production of graphene using physico-chemical methods such as epitaxial growth on silicon carbide or metal substrate had been reported. However, such methods produce lower yields, defect induced and unusual properties. Therefore, research on high yielding synthesis methods has got immense importance for the production of graphene. Several processes have been developed to synthesize single and few layer of graphene based on the exfoliation of graphite, chemical or thermal reduction of GO, chemical vapor deposition (CVD), intercalative expansion of graphite and epitaxial growth. The chemical reduction of graphite oxide (GO) to graphene or reduced graphene oxide (RGO) has been a challenging subject of research over a period of time. Strong and toxic reducing agents and surfactants play a crucial role to complete the reduction of GO in an aqueous medium. However, sodium borohydride, hydrazine and their derivatives are highly toxic and explosive. In order to overcome this problem, many attempts have been made to develop a novel aqueous and environmental friendly reduction procedures by using bacterial respiration, ascorbic acid, potassium hydroxide, polyvinylpyrrolidone, polyallylamine, baker's yeast proteins *etc*. [8-17]. With this motivation, we used pollen grains (Pgs) to produce high quality and defect free graphene sheets. The pollen grains are a reproductive cell of a plant and environmental friendly reducing agent. It also can be used as a biotemplate for the synthesis of many materials [18]. The plant *Peltophorum pterocarpum* is an ornamental tree, abundant in Indian

2

subcontinent and its Pgs were used as a reducing agent for GO in two different procedures. Efficiency of reduction by Pgs is compared with the GO prepared by using without and with hydrazine hydrate as reducing agent. Thorough structural, microstructural and electrochemical behaviour of these RGOs were studied and reported.

2. Materials and Methods

2.1 Synthesis of GO

The GO was prepared from the natural graphite flakes by a modified Hummers method [19,20]. A mixture of 2 *g* of graphite flakes in 50 *ml* of concentrated sulfuric acid in a flask was sonicated for 1 h in an ultrasonic water bath. It was then stirred for 2 *h* and cooled down to 0°C in an ice bath. Then, 5 *g* of $NaNO_3$ and 7.3 *g* of $KMnO_4$ were added in small portions to the solution which turned its color to dark greenish. When the addition was completed, temperature of the reaction mixture was raised to 35 °C under constant stirring. After 2 *h*, it was quenched by adding 200 *ml* of ice water and stirring was continued for another 6 *h*. Color of the solution has changed from dark greenish to dark brown. In order to eliminate the excess content of $KMnO_4$ and MnO_2, 7 *ml* of H_2O_2 was added and the color has changed from dark brown to light yellowish green. The resultant GO was filtered and washed with HCl (3%) and water for several times and vacuum dried at 40°C for 24 *h* to obtain the GO powder.

2.2 Synthesis of RGO

2.2.1 Synthesis of RGO using hydrazine hydrate

Exfoliation of GO to graphene oxide was done by mixing 35 *mg* of GO in 100 *ml* of water followed by ultrasonication for 3 *h* to make a homogeneous brown dispersion. In order to chemically reduce the graphene oxide to RGO, 1.5 *ml* hydrazine hydrate was added to the homogeneous dispersion followed by the addition of 10 *ml* aqueous ammonia. The reactant mixture was then heated in an oil bath at 120 °C in a water-cooled condenser for 30 *h*. Finally, the RGO was vacuum filtered and dried in vacuum oven at room temperature (RT) for overnight [21]. This sample is referred as HRGO.

2.2.2 Synthesis of RGO by using Pgs

3

The Pgs collected from the tree *Peltophorum pterocarpum* (from the campus of Pondicherry University, India) were dried in natural light for a few hours and used as such without any further treatment. The RGO was prepared by using Pgs by two methods. In the first method, 0.08 *g* of Pgs was mixed with the graphene oxide solution and sonicated for 10 *min* followed by 24 *h* of stirring at RT. The reaction temperature was then raised to 120 °C so that the solution was evaporated by leaving RGO powder which looked black in color. This sample was heat-treated at 450°C for 1.5 h in Ar gas environment to remove the unreacted Pgs. The product is free of Pgs and this sample is referred as PRGO1. The second method was similar to the PRGO1 preparation but instead of 24 h stirring at room temperature, the reactant solution (graphene oxide + Pgs) was refluxed at 120 °C for 30 *h*. The final product was vacuum filtered and dried for overnight at RT and heat-treated at 550°C for 2 h in Ar gas environment to remove the remaining Pgs. This RGO will be referred as PRGO2. For comparing the role of Pgs in the reduction of GO, the RGO was prepared without any reducing agent with similar process of HRGO and it is referred as WRGO.

2.3 Characterization

Structural phase analysis of GO and RGOs was carried out by recording the x-ray diffraction (XRD) pattern in a powder x-ray diffractometer (Rigaku, Ultima-IV) in reflection mode by using Cu-K$_{\alpha1}$ (1.5406 Å) radiation in a θ-2θ geometry (step size – 0.02°; data range – 5 – 50°; integration time – 1s). Raman spectroscopy was carried out in a laser confocal Raman microscope (Renishaw, UK, Model: Invia) by using a laser excitation wavelength of λ_{ex} = 514 nm. Microstructure was studied by scanning electron microscopy (SEM) (Quanta, FESEM, FEI) and transmission electron microscopy (TEM) (Libra 200FE, Carl Zeiss). The operating voltages for SEM and TEM were 30 and 200 kV respectively. Since graphene is conducting by itself, no conductive coatings were used for SEM measurements. Specimen for TEM measurements were prepared by dispersing the RGO samples in ethanol followed by ultrasonication and drop casting it on a copper TEM grid without support film. Elemental analysis was performed by electron energy loss spectroscopy (EELS) conducted in the TEM microscope equipped with the in-column Ω-filter. Fourier transform infrared spectroscopy (FTIR) was performed (Thermo scientific, Model: Nicolet iS10) on the graphene:KBr pellet. For electrochemical measurements, the samples were prepared by mixing them with N-Methyl-2-pyrrolidone (NMP) and isopropyl alcohol to make it in a syrupy form and they were coated on the glassy carbon electrode (GCE, CH Instruments Inc.) of 3 mm diameter

and dried in air. Cyclic voltammetry (CV) measurements were carried out in the potentiostat/galvanostat (Solartron 1287A) in a three electrode configuration with Ag/AgCl as reference electrode and Pt as counter electrode for five different scan rates (5, 10, 20, 40 and 50 mVs^{-1}) in the potential window from -1 to +1 V. Data analysis of the CV curves were done by using a Corrview software supplied along with the equipment.

3. Results and discussion

Figure 1 shows the powder XRD patterns of GO and RGO samples. Usually, the pristine graphite shows a diffraction peak at 26.6° along (002) plane with a *d*-spacing of 3.4 Å [22]. If the graphite is oxidized and turns to GO, the diffraction plane (002) of graphite is expected to disappear and shifted to 10.14° with a *d*-spacing of 8.7 Å. This increase in *d*-space is due an introduction of a large number of oxygen containing functional groups on the surface and in between the graphite sheets. Figure 1a shows the XRD pattern of GO and a diffraction peak at 10.14° confirms the formation of GO. Implantation of functional groups in between the graphite sheets overcomes the inter-sheet Van der Waals forces and enlarges the interlayer spacing [11,22]. The XRD pattern of HRGO is presented in Fig. 1b. A broad peak at 23.66° and a small peak at 42.88° are observed corresponding to (002) and (100) planes of graphene (RGO) respectively. Hydrazine hydrate is known to be a good reducing agent which reduced the GO. The XRD patterns of PRGO1 and PRGO2 are presented in Figs. 1c and 1d respectively. A broad diffraction peak corresponding to the (002) plane of RGO is appeared at ~ 20° in the case of PRGO1 and the same is appeared at 25.66° for PRGO2. The XRD patterns for the HRGO, PRGO1 and PRGO2 shown in Fig. 1 look similar to each other with a slight shift in the case of PRGO1. Therefore, the structural quality of PRGO1 and PRGO2 is almost the same as that of HRGO. Thus the XRD results confirm the complete and efficient reduction of GO by Pgs. The XRD pattern for the WRGO is presented in Fig. S1 of electronic supplementary information (ESI) and that shows an incomplete reduction evidenced from the unidentified peaks appeared at 15.88° and 12.08°. This implies the important role of Pgs in the reduction of RGO.

5
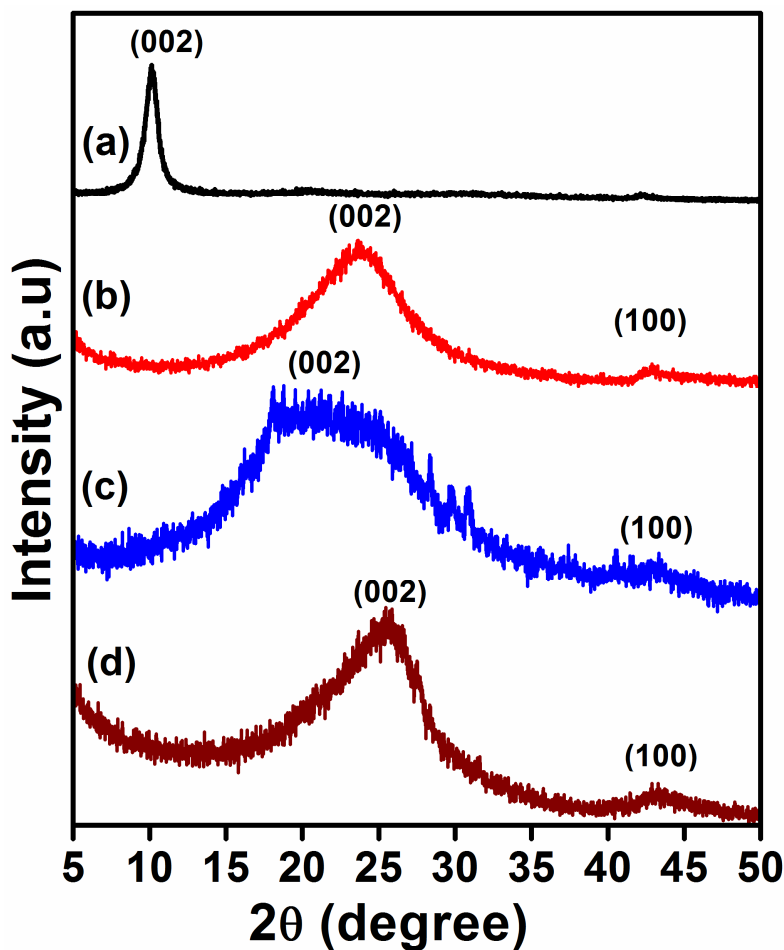
Fig. 1 X-ray diffraction patterns for the (a) GO, (b) HRGO, (c) PRGO1 and(d) PRGO2.

Figure 2 shows the FTIR transmittance spectra of GO, HRGO, pure Pgs (marked as grains), PRGO1 and PRGO2. The spectrum of Pgs is taken as control spectrum to be compared with the same of PRGOs. A broad peak occurs in the range from 3000 to 3700 cm^{-1} centered at 3420 cm^{-1} is caused by a stretching vibration of -OH of adsorbed water molecules. The IR band observed at 1651 cm^{-1} in GO and HRGO is due to bending vibrations of -OH in water molecules. The bands observed at 1734 and 1068 cm^{-1} are due to the stretching vibrations of C=O and C-O bonds of -COOH groups respectively [22,23]. The bands at 1500 and 1600 cm^{-1} have been attributed to the C=C bond vibration [23] and the peak at 1576 cm^{-1} indicates the C=C bond. Existence of these oxygen-containing groups reveals the graphite is oxidized. These polar groups, especially the surface hydroxyl groups lead to an easy formation of hydrogen bonds between graphite and water molecules and this can further explain why GO has good hydrophilicity. The other functional groups present in the HRGO, PRGO1 and PRGO2 are also marked in the FTIR spectra in Fig. 2. It is to be noted that the presence of

6

oxygen in all these samples (HRGO, PRGO1 and PRGO2) is also confirmed by EELS which will be discussed later.

It is necessary to understand the constituents of the Pgs and to know what causes the reduction. The Pgs of *Peltophorum pterocarpum* have been studied for their constituents by sodium dodecyl sulphate polyacrylamide gel electrophoresis (SDS-PAGE) [24]. The crude extract of the Pgs were identified to contain 20 protein bands (by Lowry's Method) with a molecular weight ranging from 17 to 98 kDa. By performing the periodic acid-Schiff (PAS) staining, three bands at 98, 76, and 66 kDa corresponding to glycoproteins were found [24]. These glycoproteins have done a job of reducing GO to PRGO1 and PRGO2 in this study. There are reports available [25] on the reduction of GO by plant extracts which were proved to contain biomolecules such as proteins, amino acids, vitamins and enzymes. These biomolecules present in the plant extract have played a role of reduction systems and reduced GO [32]. Presence of these electron rich functional groups was confirmed by FTIR studies. The FTIR spectrums for the Pgs were analyzed in comparison with the reported results [25]. The FTIR bands corresponding to amide I (1656 cm^{-1}), amide II (1546 cm^{-1}) and amide III (1252 cm^{-1}) are observed in the Pgs used in this work (see the FTIR spectrum of "grains" in Fig. 2). After confirming the presence of these electron rich functional groups in Pgs, it can be concluded that the reducing biomolecule protein groups present in the Pgs of *Peltophorum pterocarpum* have played a role in the reduction of GO to RGO (PRGO1 and PRGO2).

7
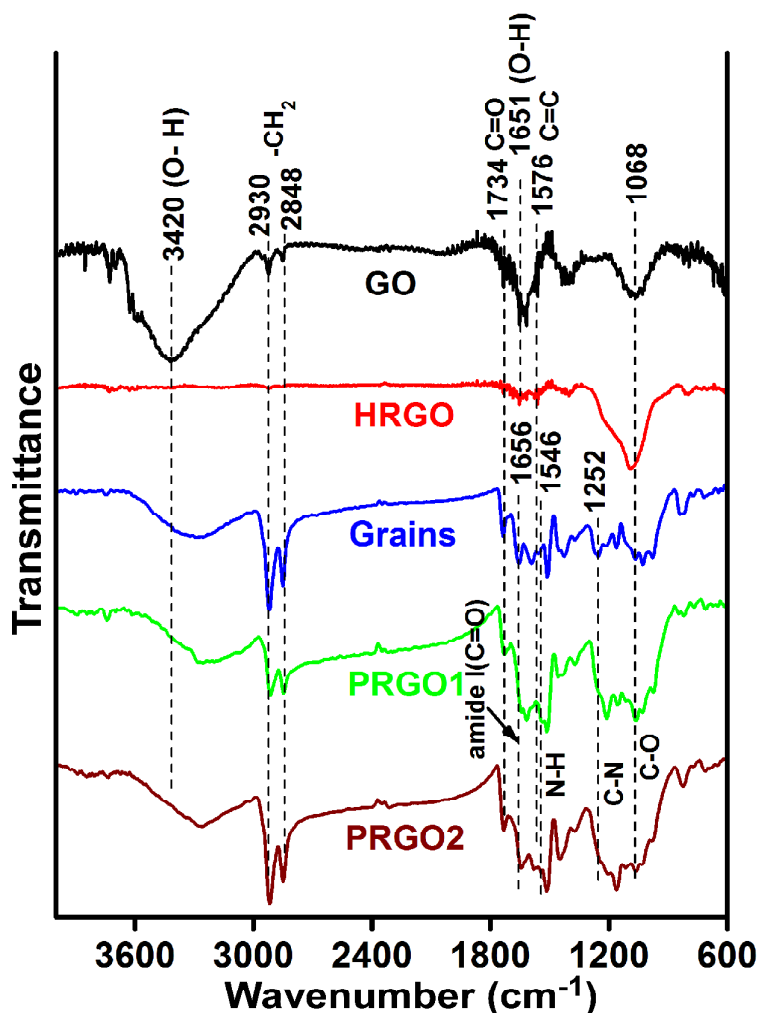
Fig. 2 The FTIR transmittance spectra of GO, HRGO, Pgs, PRGO1 and PRGO2.

Raman spectra of GO, HRGO, PRGO1 and PRGO2 are presented in Fig. 3. Usually, a Raman peak of natural graphite occurs at 1574 cm^{-1} which is known as the G band and a characteristic peak of a single crystal graphite caused by a stretching vibration of sp^2 type C-C bonds. The Raman peak at 1350 cm^{-1} is a D band caused by grain size, as well as the disordered structures and defects of graphite, i.e., by double-resonance Raman scattering. In addition, a peak at 2725 cm^{-1} is the 2D band of natural graphite [26]. The Raman spectrum of GO in Fig. 3 shows two Raman peaks at 1355 and 1597 cm^{-1} corresponding to D and G bands respectively. Intensity ratio of D to G band (I$_D$/I$_G$) is obtained to be 0.8 which confirms the formation of GO. When compared to graphite, the D and G Raman bands in GO are broadened and shifted to 1355 and 1597 cm^{-1} indicating the oxidation of graphite. In the case of HRGO, the D and G bands are observed at 1349 and 1587 cm^{-1} respectively. Similar features are also observed in the case of PRGO1 and PRGO2. In the cases of HRGO, PRGO1

8

and PRGO2, the D and G bands were shifted closer to the peak position of graphite indicating the reduction of GO. The intensity ratio I_D/I_G changes from 0.8 (GO) to 1.35 (HRGO). For PRGO1 and PRGO2, the intensity ratio is 0.93 and ~0.87 respectively, and these values are higher than that of GO, indicating an increase in the average size of the sp^2 domain upon the reduction of GO [27].
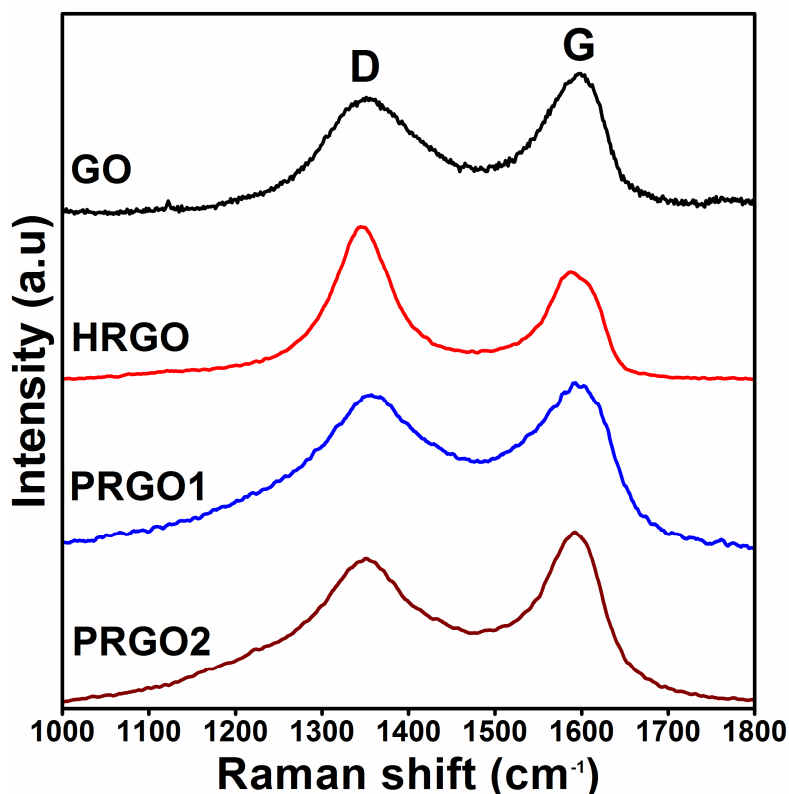

Fig. 3 Raman spectra of GO, HRGO, PRGO1 and PRGO2 acquired with the laser excitation of λ_{ex} = 514 nm.

Microscopic studies for the Pgs using SEM shows that their microstructure has tricolporate aperture and reticulate ornamentation and the shape is oblate spheroidal. Typical SEM images of the Pgs are presented in Fig. 4 and similar morphology was already reported [24]. Figure 5 shows the low and high magnification SEM micrographs in pair for GO in Fig. 5a & 5b, HRGO in Fig. 5c & 5d, PRGO1 in Fig. 5e & 5f and PRGO2 in Fig. 5g & 5h. Figures 5a and 5b clearly show that the GO has formed like bundles and not well exfoliated. The HRGO samples are well exfoliated as expected and this can be seen in Fig. 5(c) and 5(d). The SEM images of PRGO1 and PRGO2 without annealing are presented Fig. S2 of ESI, which shows the presence of Pgs along with the RGO sheets in both the cases. These Pgs were removed by

heating as explained in the experimental. The SEM images of PRGO1 and PRGO2 after heat treatment are shown in Figs. 5e & 5f and 5g & 5h respectively. It is seen clearly that all of them have a well exfoliated graphene sheets.
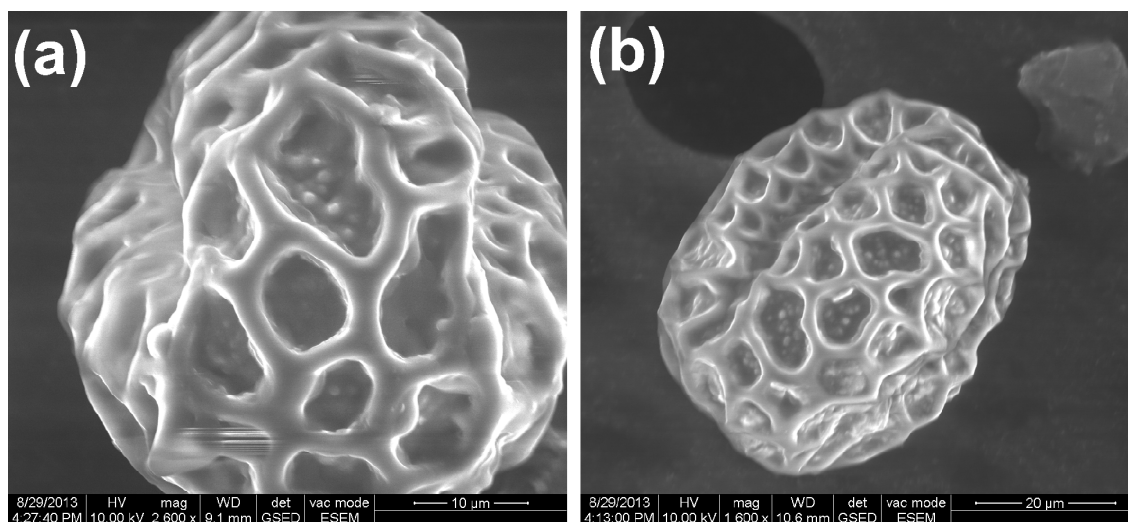
Fig. 4 FESEM micrograph of pollen grains of *Peltophorum pterocarpum* shows (a) tricolporate aperture and reticulate ornamentation and (b) oblate spheroidal. These images were acquired in E-SEM mode without any conductive coating on the Pgs.

10
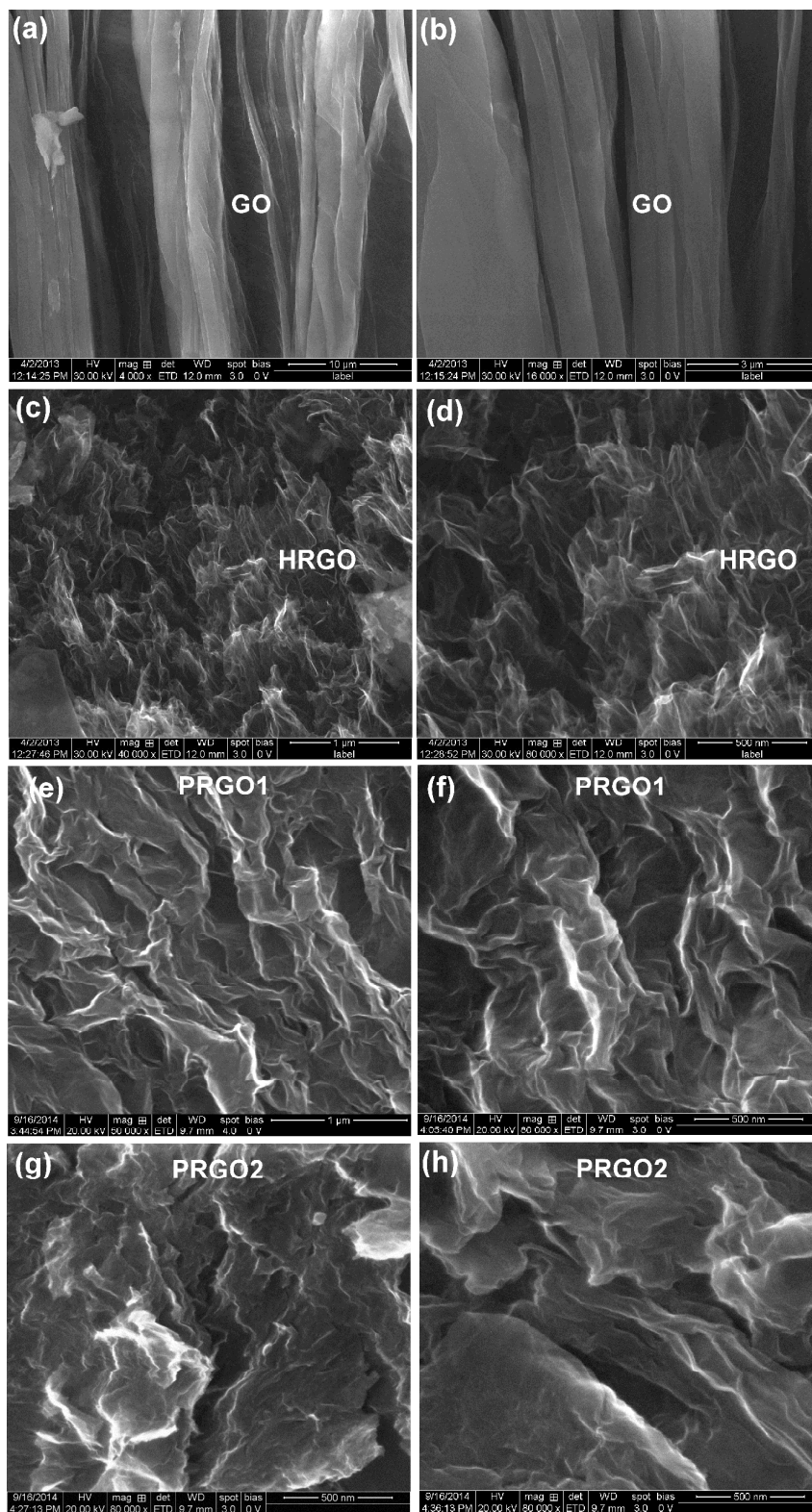
Fig. 5. Low and high magnification FESEM micrographs of (a, b) GO, (c, d) HRGO, (e, f) PRGO1 and (g, h) PRGO2. Left and right are the low and high magnification images

respectively. Vertical and horizontal arrows (e) show the RGO and Pgs respectively in PRGO1. The inset of (e) shows the single pollen grain with the RGO on top.

Composition analysis of the PRGO1 and PRGO2 was performed by energy dispersive spectroscopy carried out in the SEM microscope. The EDS spectra for PRGO1 and PRGO2 are presented in Fig. S3 of the ESI and they show that the dominant presence of C with a trace of oxygen. No other impurity elements were found.

Bright field TEM micrographs of the HRGO, PRGO1 and PRGO2 are presented in Fig. 6a, 6b and 6c respectively. The selected area electron diffraction (SAED) patterns are presented as inset in the respective TEM images. Wrinkles and folds are seen in the graphene sheets in all the three samples and these are the signatures of the well exfoliated single graphene sheets. The SAED patterns show sharp rings indicating a short range ordered HRGO and PRGO1. But diffraction spots seen in the SAED of PRGO2 confirms better crystalline nature. Core loss EELS spectra for the C-K edges of all the RGOs samples are presented in Fig. 6(d). The background subtraction of the EELS spectra was carried out by using a standard power law function $I = A. E^{-r}$, where A and r are the fitting parameters [28]. Shape of the C-K edge was analyzed in comparison with the C-K edge data for graphite, amorphous carbon and graphene oxide which describes the atomic and electronic structure of graphene oxide by EELS experiment and density of states calculations [29]. The other detailed report on graphene by EELS was also used for comparative analysis of the observed C-K ionization edge [30,31]. The peaks marked as A and B in Fig. 6(d) correspond to the π^* and σ^* electronic transitions respectively for graphene. Fine structures of the C-K ionization edge of RGOs are exactly matches with the graphene [30,31]. The other two phases such as graphite and amorphous carbon have completely different fine structures [29]. It is also important to note that the shape of the C-K EELS spectrum of GO is different from the graphene. The difference in the fine structures of GO and HRGO is compared and presented in the inset of Fig. 6d. In corroboration with the results reported earlier [29-31], it can be concluded that the formed carbon phase is RGO in all the three cases of HRGO, PRGO1 and PRGO2. However, a signature of oxygen is also found in the RGO samples and the oxygen K-edge of these samples are present in Fig. 7 and this result is in consistent with the C-O and C=O bands observed in FTIR. These results confirm the well-formed RGO phase by the Pgs. By taking into account of all the above discussed results (XRD, FTIR, Raman, SEM and TEM), Fig. 8
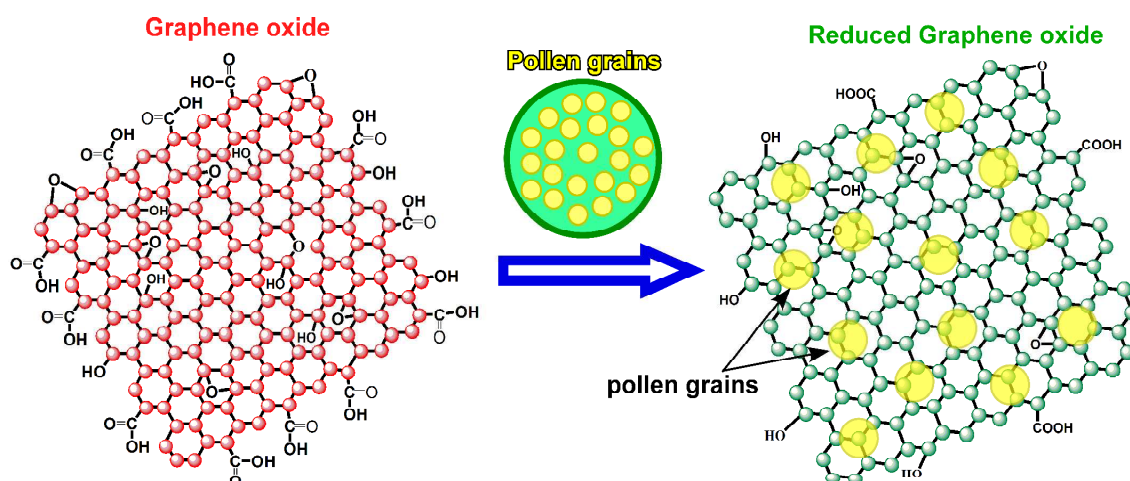
presents the schematic illustration for the reduction of GO by pollen grains of *Peltophorum pterocarpum*.
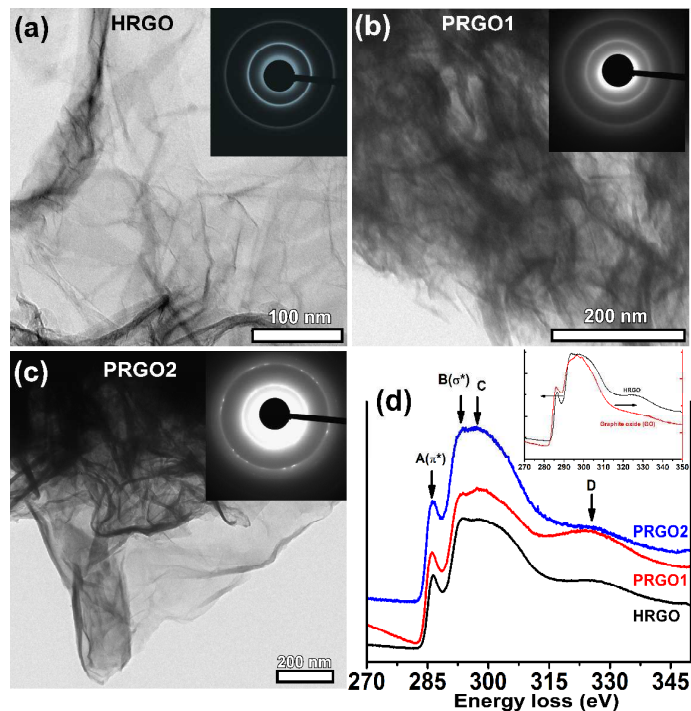
Fig. 6 The bright field TEM images of (a) HRGO, (b) PRGO1, (c) PRGO2 and (d) the EELS spectra of HRGO, PRGO1 and PRGO2 samples. Inset of the TEM images are the corresponding SAED patterns of the respective samples. The inset of (d) is the comparison between the EELS fine structures of GO and HRGO. Background subtraction of the core-loss EELS spectra was performed by using the power law function.
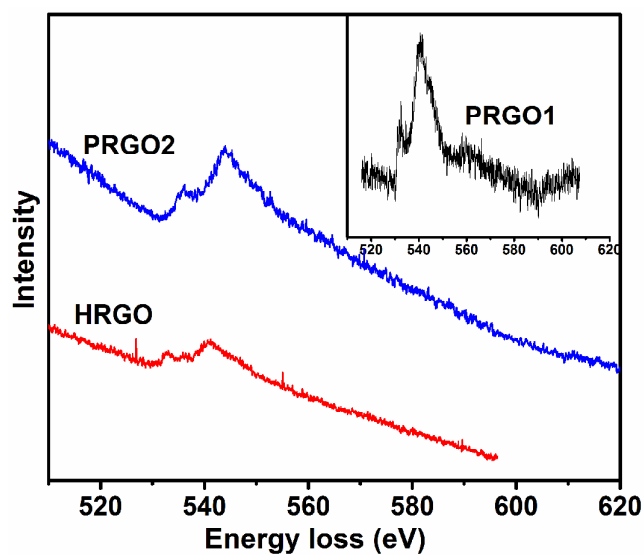
Fig. 7 The O-K core loss EELS spectra of reduced graphene HRGO, PRGO1 (inset) and PRGO2. The spectra are presented as such without any process. Background subtraction of the core-loss EELS spectra was performed by using the power law function.

Fig. 8 Schematic illustration for the reduction of GO to RGO by the Pgs of *Peltophorum pterocarpum*. The electron rich functional groups present in the biomolecules of the Pgs are the cause for the reduction of GO

Figures 9(a), 9(b) and 9(c) present the respective cyclic voltammograms of HRGO, PRGO1 and PRGO2 acquired for five different scan rates of 5, 10, 20, 40 and 50 mVs^{-1}. The electrolyte used was 0.5 M of Na_2SO_4 with the potential window of -1 to +1 V. The GCE/sample combination was used as a working electrode. Area under the CV cycle is found to increase with increasing scan rate which is expected. The CV curves of all the RGOs show a quasi-rectangular shape due to the increase in current with the applied voltage. The specific capacitance (Fg^{-1}) of the RGOs were calculated from half of the integrated area (*I*d*V*, in Coulomb/s.V) of the CV curves by using the formula,

$$\text{Specific Capacitance } (Fg^{-1}) = \frac{\text{Area } (C/s \cdot V)}{\text{scan rate } (mV/s) \times \text{Voltage window } (V) \times \text{mass } (g)} \qquad (1).$$
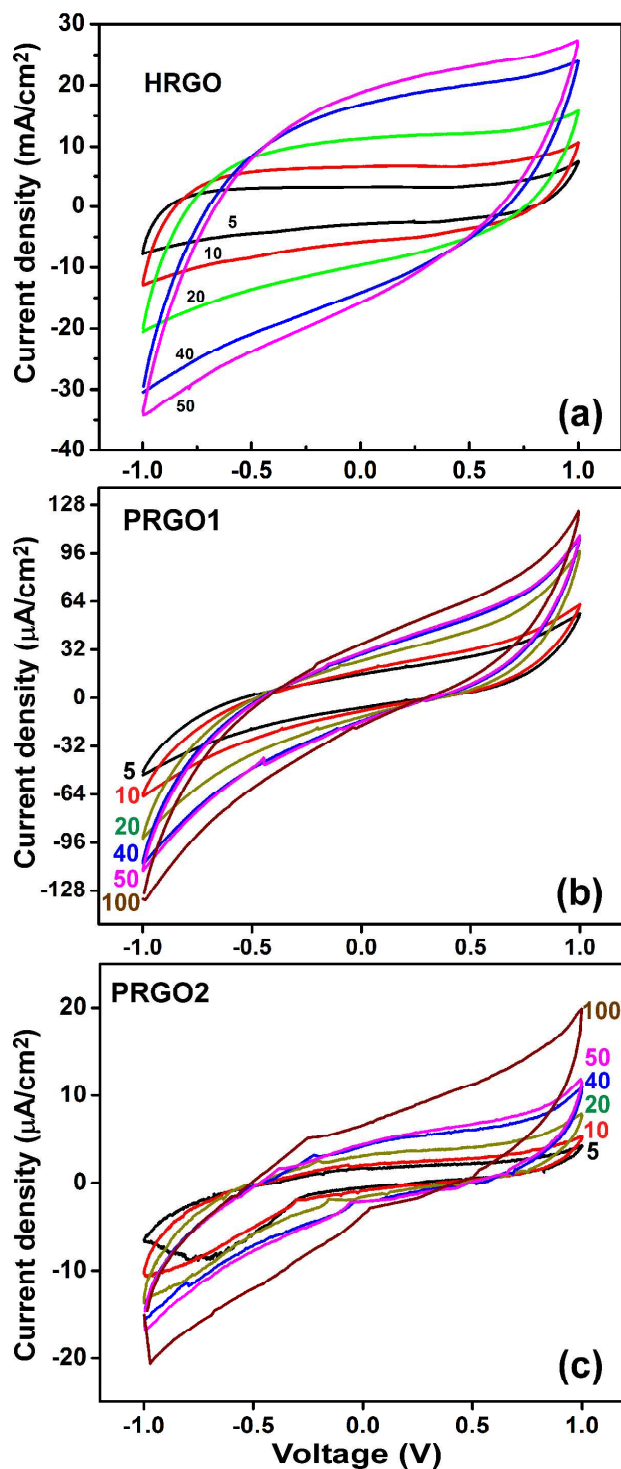
Fig. 9 Cyclic voltammograms of (a) HRGO, (b) PRGO1 and (c) PRGO2 acquired at different scan rates. The number marked in the CV curves denotes the scan rate in mV s^{-1} with which the data were acquired. Three electrode configurations with GCE/RGO as working electrode, Ag/AgCl as reference electrode and Pt as counter electrode with 0.5M Na$_2$SO$_4$ solution as electrolyte.

The specific capacitance values obtained for the HRGO, PRGO1 and PRGO2 for different scan rates are presented in Table 1. The specific capacitance of HRGO, PRGO1 and PRGO2 lies in the range of 480.4–214.8 Fg[-1], 27.1–3.1 Fg[-1] and 4.8 to 0.9 Fg[-1] respectively for the scan rate varied from 5 to 100 mVs[-1]. Specific capacitance of PRGO1 is 15.7 Fg[-1] for the scan rate of 10 mVs[-1] and it is quite comparable to the reported values [32], which is 17 to 21 Fg[-1]. The PRGO2 gives relatively lower specific capacitance of 2.8 Fg[-1] for the scan rate of 10 mVs[-1].

Table 1. Specific capacitance of HRGO, PRGO1 and PRGO2 obtained from cyclic voltammograms acquired for five different scan rates (from Eqn. (1))

Samples/Scan rate (mV s^{-1})	Specific capacitance (Fg[-1])					
	5	10	20	40	50	100
HRGO	480.4	454.7	356.4	246.6	214.8	-
PRGO1	27.1	15.7	11.0	6.4	5.2	3.1
PRGO2	4.8	2.8	1.9	1.2	1.2	0.9

Figure 10 shows the plot of maximum current (I_{max}) versus square root of the scan rate ($v^{1/2}$) for HRGO, PRGO1 and PRGO2. The maximum current for the HRGO, PRGO1 and PRGO2 was taken from the peak of the positive potential. All the plots were fitted with linear function. The linear dependence of the capacitive current with square root of the scan rate shows a double layer capacitor like behavior for these RGOs [33].
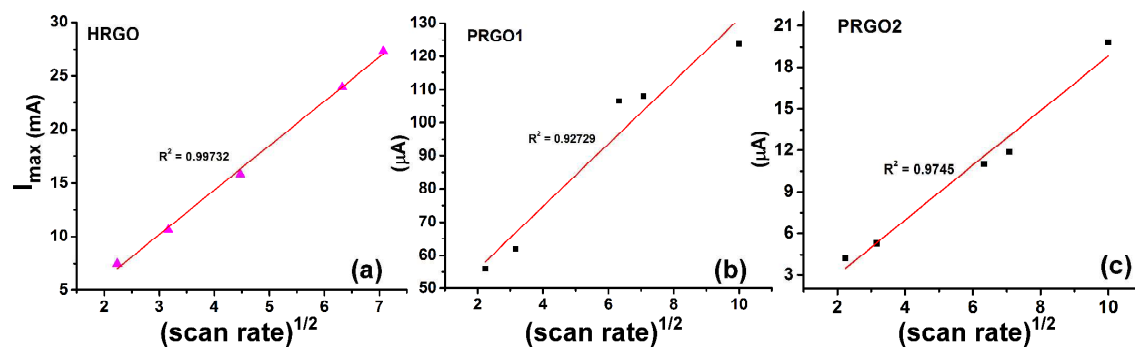
Fig. 10 Plot of maximum current (I_{max}) versus square root of the scan rate obtained from the CV curves for (a) HRGO, (b) PRGO1 and (c) PRGO2.

4. Conclusion

Green synthesis method with cost effective way of reducing GO to RGO by using the Pgs of *Peltophorusm pterocarpum* is demonstrated. The Pgs were neither bought from any company nor processed but used as-received from the plant and therefore the preparation cost has down significantly. The product is compared with the one obtained by using hydrazine hydrate, the latter was being used as a control sample. Pollen grains have reduced the GO but not comparable with hydrazine hydrate which is the best reducing agent for the preparation of graphene. The RGOs were thoroughly studied for their structure and microstructure showing a good exfoliation by this method. The specific capacitance of the reduced graphene oxide by the Pgs is 27.1 Fg^{-1} (scan rate of 5 mVs^{-1}) and this is quite comparable to the already reported values for the RGO prepared by using bio-routes. The overall conclusion is that the Pgs of *Peltophorum pterocarpum* can effectively be used to prepare the RGOs without environmental hazards and the RGO can be useful to make bilayer capacitors.

References

1. Geim AK, MacDonald AH (2007) Graphene: Exploring Carbon Flatland, Phys Today 60:35-41.

2. Orlita M, Faugeras C, Plochocka P, Neugebauer P et al (2008) Approaching the Dirac point in high mobility multi-layer epitaxial graphene, Phys Rev Lett 101:267601-267604.

3. Liu Y, Dong X, Chen P (2012) Biological and chemical sensors based on graphene materials, Chem Soc Rev 41:2283-2307.

4. Bonaccorso F, Sun Z, Hasan T, Ferrari AC (2010) Graphene photonics and optoelectronics, Nature photonics 4:611-622.

5. Bunch JS, van der Zande AM, Verbridge SS, Frank IW et al (2007) Electromechanical Resonators from Graphene Sheets, Science 315:490-493.

6. Perera SD, Liyanage AD, Nijem N, Ferraris JP et al (2013) Vanadium oxide nanowire-Graphene binder free nanocomposite paper electrodes for supercapacitors: A facile green approach, J Power Sources 230:130-137.

7. Xia J, Chen F, Li J, Tao N (2009) Measurement of the quantum capacitance of graphene, Nat Nanotechnol 4:505-509.

8. Schmidt EW (2001) *Hydrazine and its Derivatives* Wiley-Interscience, New York

9. Stankovich S, Dikin DA, Piner RD, Kohlhaas KA et al (2007) Synthesis of graphene based nanosheets via chemical reduction of exfoliated graphite oxide, Carbon 45:1558-1565.

10. Yang D, Velamakanni A, Bozoklu G, Park S et al (2009) Chemical analysis of graphene oxide films after heat and chemical treatments by x-ray potoelectron and micro-raman spectroscopy, Carbon 47:145-152.

11. McAllister MJ, Li J-L, Adamson DH, Schniepp HC et al (2007) Single sheet functionalized graphene by oxidation and thermal expansion of graphite, Chem Mater 19:4396-4404.

12. Fan X, Peng W, Li Y, Li X et al (2008) Deoxygenation of exfoliated graphite oxide under alkaline conditions: A green route to graphene preparation, Adv Mater 20:4490-4493.

13. Ai K, Liu Y, Lu L, Cheng X et al (2011) A novel strategy for making soluble reduced graphene oxide sheets cheaply by adopting an endogenous reducing agent, J Mater Chem 21:3365-3370.

14. Gurunathan S, Han JW, Eppakayala V, Kim J (2013) Microbial reduction of graphene oxide by Escherichia coli: A green chemistry approach, Colloids and surfaces B: Biointerfaces 102:772-777.

15. Akhavan O, Ghaderi E (2012) *Escherichia coli* bacteria reduce graphene oxide to bactericidal graphene in a self-limiting manner, Carbon 50:1853-1860.

16. Wang G, Qian F, Saltikov CW, Jiao Y et al (2011) Microbial reduction of graphene oxide by *shewanella*, Nano Res 4(6):563-570.

17. Salas EC, Sun Z, Luttge A, Tour JM (2010) Reduction of graphene oxide via bacterial respiration, ACS Nano 4(8):4852-4856.

18. Song F, Su H, Han J, Lau WM et al (2012) Bioinspired Hierarchical Tin Oxide Scaffolds for Enhanced Gas Sensing Properties, J Phys Chem C 116:10274-10281.

19. Hummer WS, Offeman RE (1958) Preparation of graphite oxide, J Am Chem Soc 80:1339.

20. Hu N, Gao R, Wang Y, Wang Y et al (2012) The preparation and characterization of non-covalently functionalized graphene, J Nanosci Nanotechnol 12(1):99-104.

21. Li D, Muller MB, Giljie S, Kaner RB et al (2008) Processable aqueous dispersions of graphene nanosheets, Nat Nanotechnol 3:101-105.

22. Kaniyoor A, Baby TT, Ramaprabhu S (2010) Graphene synthesis via hydrogen induced low temperature exfoliation of graphite oxide, J Mater Chem 20:8467-8469.

23. Bagri A, Mattevi C, Acik M, Chabal YJ et al (2010) Structure evolution during the reduction of chemically derived graphene oxide, Nat. Chem 2:581-587.

24. Mandal J, Roy I, Gupta-Bhattacharya S (2011) Clinical and immunobiochemical characterization of airborne Peltophorum pterocarpum (yellow gulmohar tree) pollen: a dominant avenue tree of India, Ann Allergy Asthma Immunol 106:412-420.

25. Mhamane D, Ramadan W, Fawzy M, Rana A et al (2011) From graphite oxide to highly water dispersible functionalized graphene by single step plant extract-induced deoxygenation, Green Chem13:1990-1996.

26. Malard LM, Pimenta MA, Dresselhaus G, Dresselhaus MS (2009) Raman spectroscopy in graphene, Phys Rep 473:51-87.

27. Cheng W, Yan L (2012) Centimeter-sized dried foam films of Graphene: Preparation, Mechanical and Electronic Properties, Adv Mater 24(46):6229-6233.

28. Egerton RF (2011) *Electron Energy Loss Spectroscopy in the Electron Microscope* (3rd edn). Plenum Press, New York, pp 260-264

29. Mkhoyan KA, Contryman AW, Silcox J, Stewart DA et al (2009) Atomic and Electronic Structure of Graphene-Oxide, Nano Lett 9(3):1058-1063.

30. Dato A, Frenklach M (2010) Substrate-free microwave synthesis of graphene: experimental conditions and hydrocarbon precursors, New J Phys 12:125013:1-24.

31. Dato A, Radmilovic V, Lee Z, Phillips J et al (2008) Substrate-Free, Gas-Phase Synthesis of Graphene Sheets, Nano Lett 8(7):2012-2016.

32. Thakur S, Karak N (2012) Green reduction of graphene oxide by aqueous phytoextracts, Carbon 50:5331-5339.

33. Liu A, Li C, Bai H, Shi G (2010) Electrochemical Deposition of Polypyrrole/Sulfonated Graphene Composite Films, J Phys Chem C 114:22783-22789.